

# Physical and Chemical Properties of Rice Husk Ash Concrete Under Seawater

Ramadhansyah Putra Jaya<sup>1\*</sup>, Mohd Rosli Hainin<sup>2</sup>, Mohd Haziman Wan Ibrahim<sup>3</sup>, Fadzli Mohamed Nazri<sup>4</sup>, Mohd Fadzil Arshad<sup>5</sup>, Khairunisa Muthusamy<sup>1</sup>

<sup>1</sup>Faculty of Civil Engineering and Earth Resources, Universiti Malaysia Pahang, 26300 Gambang, Pahang, Malaysia

<sup>2</sup>Faculty of Engineering, School of Civil Engineering, Universiti Teknologi Malaysia, 81310 UTM Skudai, Johor Bahru, Malaysia

<sup>3</sup>Faculty of Civil and Environmental Engineering, Universiti Tun Hussein Onn Malaysia, 86400 Batu Pahat, Johor Bahru, Malaysia

<sup>4</sup>School of Civil Engineering, Universiti Sains Malaysia, 14300 Nibong Tebal, Penang, Malaysia

<sup>5</sup>Faculty of Civil Engineering, Universiti Teknologi Mara, 40450 Shah Alam, Selangor, Malaysia

Received 22 March 2018; accepted 2 October 2018, available online 24 October 2018

**Abstract:** The physical and chemical properties of rice husk ash concrete under seawater attack are evaluated based on thermogravimetric analysis, X-ray diffraction, and scanning electron microscopy. A rice husk ash (RHA) dosage of 10% by weight of binder was used throughout the experiments. The results clearly showed that RHA can be satisfactorily used as a cement replacement material in order to increase the durability of concrete under seawater attack. The used of RHA as cement replacement in concrete reduced the quantities of ettringite and gypsum formation. The results indicated that blended cement prepared with RHA reduced the potential for the formation of ettringite and gypsum due to the reduction in the quantity of calcium hydroxide and C<sub>3</sub>A, and thus improved the resistance of concrete to seawater attack. Furthermore, more formation of ettringite and gypsum was observed from Portland cement concrete compared to the RHA blended cement. Finally, it can be concluded that calcium hydroxide (Ca(OH)<sub>2</sub>) can be reduce when ground RHA is used as partially replacement cement.

**Keywords:** Physical, Chemical, Concrete, Seawater, Rice husk ash

## 1. Introduction

The deterioration of concrete in marine environment has been a topic of interest to concrete technologists in the past few decades [1]. In a marine environment, chloride and sulfate ions penetrate into the concrete through seawater attack [2-4]. Generally, chloride ions are attributed to the formation of Friedel's salt [5], whereas the sulfate ions react with portlandite to form gypsum, which reacts with hydrated calcium aluminate to produce secondary ettringite [6]. Rice husk ash, fly ash, silica fume, palm oil fuel ash and slag are good pozzolanic materials to be used in concrete [7-9]. These mineral admixtures have been widely used in severe environmental conditions, such as marine environment and ground water [10]. However, not many researches have carried out this topic to evaluate the effect of RHA blended cement in seawater attack, especially on local infrastructure in the context of Malaysia. The evaluation of the effects of seawater on RHA blended cement can provide important data for the design and maintenance of infrastructures in Malaysia. In this study, the performance of RHA blended cement subjected to seawater was

investigated. RHA ground was applied throughout this investigation. Likewise, the controlled specimens (OPC) were prepared in the same batch as well.

## 2. Materials

Ordinary type I Portland cement (OPC, Blue Lion Cement) was used as the major binder in the production concrete. The chemical composition of the OPC used in this study was within the standard range of 70% CaO, 17.8% SiO<sub>2</sub>, 3.9% Al<sub>2</sub>O<sub>3</sub>, 3.2% Fe<sub>2</sub>O<sub>3</sub>, 1.5% MgO, and 3.6% SO<sub>3</sub>. The OPC similarly indicated a compound composition of 54.5% C<sub>3</sub>S, 18.2% C<sub>2</sub>S, 9.4% C<sub>3</sub>A, and 10.5% C<sub>4</sub>AF. The chemical analysis on the OPC was carried out using XRF apparatus in accordance with the procedure given in BS EN 197-1:2011 [11].

Rice husk was initially incinerated in a gas furnace at a heating rate of 10°C/min; the temperature was increased until 700°C, after which it was maintained for 6 h. After the incineration, the RHA was left inside the furnace to cool and then collected the following day. Afterwards, the RHA was ground using a laboratory ball mill with porcelain balls. SiO<sub>2</sub> was identified as the main component of the RHA. In addition, SiO<sub>2</sub>, Al<sub>2</sub>O<sub>3</sub>, and

\*Corresponding author: [ramadhansyah@ump.edu.my](mailto:ramadhansyah@ump.edu.my)  
2018 UTHM Publisher. All right reserved.  
[penerbit.uthm.edu.my/ojs/index.php/ijie](http://penerbit.uthm.edu.my/ojs/index.php/ijie)

Fe<sub>2</sub>O<sub>3</sub> comprised 93.48% of the material, in accordance with C618-15 of the American Society for Testing and Materials (ASTM) [12], which requires that these three main oxides should comprise no less than 70% of the pozzolanic material.

### 3. Methods

In this study, thermogravimetric analysis and differential thermal analysis were applied in order to observe the reactions taking place during the thermal treatment of the samples. The analysis was carried out using TA-60WS. At the specified testing, a total of 20 - 25 mg of the samples were taken in a platinum pan and heated in nitrogen atmosphere at a temperature range between 20°C to 1200°C with controlled heating rate 10°C/min. On the other hand, the pozzolanic activity index of RHA blended cement concrete was evaluated in accordance with ASTM C311 / C311M – 17 [13].

X-ray diffraction is one of the most powerful methods for characterizing crystalline materials. It can also be used to identify the phases present in samples from raw materials to the finished product. According to BS EN 13925-1:2003 [14], the samples were scanned in steps of 0.034° (2θ) with a fixed counting time of 1 second. The range of X-ray scan was from 2θ = 10° to 90° 2θ, using copper (Kα Cu) with wavelength (λ) of 1.5406 nm as X-Ray source. EVA software was used to analyze the phase of the samples.

The scanning electron microscope (SEM) is typically performed in a high vacuum because gas molecules interfere with the electron beam and with the emitted secondary and backscattered electrons used for imaging. Field Emission Scanning Electron Microscope (FESEM) was used to characterize the samples in this study. In order to determine the morphological characterization, the samples need to be cut into small sizes. The sample then needs to be horizontally placed on the substrate holder (180°) for the surface analysis and vertically at 90° for the cross-sectional view (thickness). Magnification of 5 kX, 10 kX, 20 kX, and 50 kX were used for morphology of the samples with the operation power of 3 kV and 5 kV.

### 4. Results and Discussion

The results of the TGA-DTA of specimens subjected to seawater are illustrated in Fig. 1. The curve of the specimen generally showed five endothermic peaks. The first endothermic peak, detected between 67.63 and 110.78 °C, with a peak at 82.93 °C and a 5.06% weight loss, can be associated with the dehydration of ettringite (Ca<sub>6</sub>Al<sub>2</sub>(SO<sub>4</sub>)<sub>3</sub>(OH)<sub>12</sub>·26H<sub>2</sub>O). Santhanam et al. [15] have found an endothermic peak at 80 and 100 °C due to the dehydration of ettringite, whereas Vedalakshmi et al. [16] have reported the dehydration of ettringite at around 80 and 130 °C. It can be seen that the seawater attack on concrete has been attributed to the reaction of MgSO<sub>4</sub> with Ca(OH)<sub>2</sub> liberated, forming gypsum and Mg(OH)<sub>2</sub>. The gypsum formed reacts with calcium hydroxide liberated during hydrolysis of calcium silicates and forms ettringite. In addition, the chloride present in seawater reacts with liberated Ca(OH)<sub>2</sub> as well as C<sub>3</sub>A to form

Friedel's salt. The second endothermic peak located between 100.81 and 147.04 °C, with a peak at 115.84 °C and a 2.38% weight loss, is the result of the dehydration of gypsum (CaSO<sub>4</sub>·2H<sub>2</sub>O). The test results of Li et al. [17] have shown that the dehydration of gypsum formation is indicated by an endothermic peak at 110 and 130 °C. The third endothermic peak observed between 254.70 and 362.16 °C, with a peak at 295.35 °C and 2.30% weight loss, could be attributed to the decomposition of calcium silicate hydrate (C-S-H), calcium aluminate hydrate, and Friedel's salt. Furthermore, the endothermic peak corresponding to brucite (small peak) was also identified and confirmed by DTA curve. The endothermic peak corresponding to brucite occurred at temperatures ranging between 350.10 to 400.09 °C. The weight loss corresponding to brucite was 0.73%, with a peak appearing at about 374.85 °C. The fourth endothermic peak identified in the range of 410.86 and 459.69 °C, with a peak in the region of 435.26 °C and a 3.35% weight loss, can be attributed to the dehydroxylation of the calcium hydroxide. Finally, the endothermic peak between 656.31 to 743.60 °C with a peak at around 714.83 and a 8.75% weight loss is the result of calcium carbonate (CaCO<sub>3</sub>) coming from seawater.

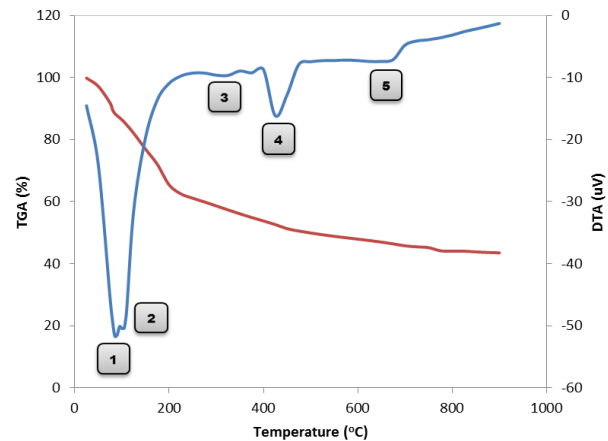
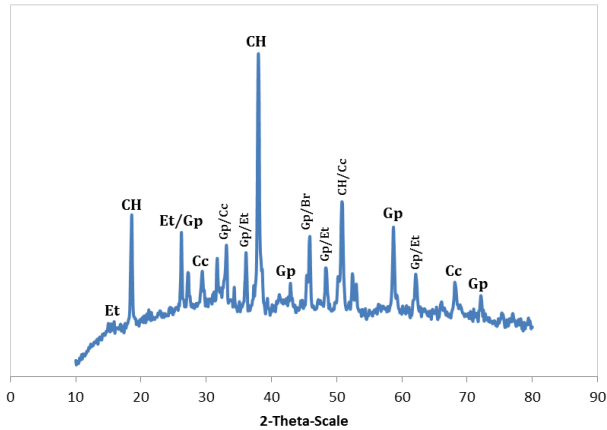


Fig. 1 TGA/DTA curve of RHA cement paste under seawater

Fig. 2 and Fig. 3 demonstrate the XRD of OPC and RHA blended cement pastes subjected to seawater. Based on Fig. 2, it can be seen that there were the relatively large intensity peaks for calcium hydroxide in no replacement RHA paste cured in seawater. Furthermore, a large quantity of calcium hydroxide was converted to gypsum or brucite (Mg(OH)<sub>2</sub>) as seen in Fig. 2. The presence of calcite phase in the examined pastes implies the carbonation effect on surface of specimens which is less in those mixes with RHA as illustrated in Fig. 3. On the other hand, ettringite phase was detected in pastes with and/or without rice husk ash. The XRD analysis also showed that gypsum and ettringite peak in each specimen was strong (Fig. 2), indicating that these formations were the main corrosion products. However, the addition of RHA in blended cement reduced the deterioration of concrete caused by seawater attack (Fig. 3). In addition,

the replacement of cement with RHA in pastes exposed to seawater had lower ettringite, gypsum, and brucite intensity peaks compared with those of the OPC paste (Fig. 3). As expected, the RHA pastes had more SiO<sub>2</sub> content than those without RHA (control specimen). The RHA is assumed to be as the reactant to produce secondary C-S-H by consuming calcium hydroxide. The formation of pozzolanic gel begins during hardening process. Decreased calcium hydroxide content of the cement matrix and increased amount of C-S-H gel together with filler effect of RHA contribute to protection of concrete against to seawater attack.



\*Et, ettringite; Gp, gypsum; CH, calcium hydroxide; Br, brucite; Cc, calcite

Fig. 2 XRD patterns of the OPC cement paste under seawater

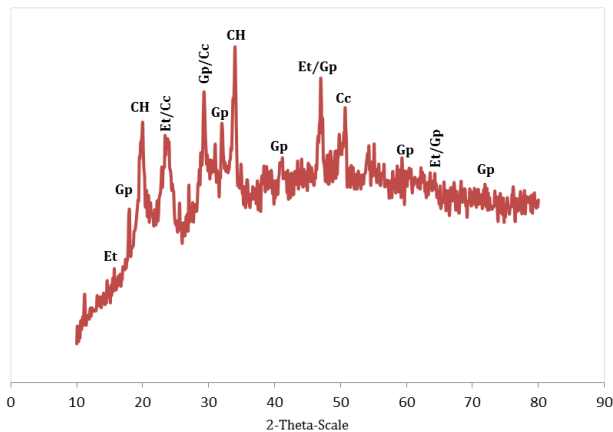


Fig. 3 XRD patterns of the RHA cement paste under seawater

The morphology of OPC and RHA blended cement pastes subjected to seawater were observed using SEM (Fig. 5 and Fig. 7). In addition, EDX analysis was conducted on samples to determine the existing compounds after reactions with seawater (Fig. 4 and Fig. 6). Based on Fig. 4, the main elements noted were magnesium (Mg), silica (Si), sodium (Na), aluminium (Al), chloride (Cl), calcium (Ca) and iron (Fe). A silica peak was easily observed which indicated the presence of C-S-H in the paste. The SEM images of OPC paste showed various microstructure formations, such as calcium hydroxide,

calcium-silicate-hydrate gel, gypsum, and ettringite (Fig. 5).

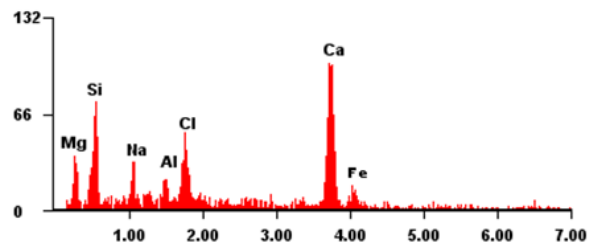


Fig. 4 EDX analysis of OPC cement paste under seawater

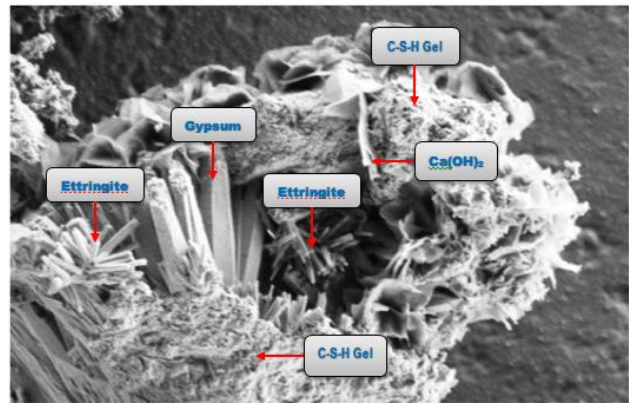


Fig. 5 Morphology of OPC cement paste under seawater

From Fig. 6, the EDX analyses showed that the Si and Ca peaks was highest than other elements. In cement chemistry, CaO, SiO<sub>2</sub>, and H<sub>2</sub>O are represented by C, S, and H respectively. On the other hand, the results also indicated that the lower peaks of magnesium hydroxide (Mg(OH)<sub>2</sub>) and chloride in RHA mixes which is attributed to the lower calcium hydroxide resulting from pozzolanic reaction. Therefore, the use of RHA in blended cement seemed to have given some protection to the deterioration of concrete even when subjected to seawater attack. Replacement of cement with RHA reduces the amount of calcium hydroxide in the paste, decreases gypsum and ettringite formation. Reduction in calcium hydroxide always leads to less gypsum and ettringite formation. Based on Fig. 7, ettringite exist as long slender needles, calcium hydroxide are precipitated as hexagonal plates, C-S-H gel exhibit a fine layered network, while the gypsum comprised elongated rod-shaped formations. C-S-H gel is believed to have a layered structure. It can be seen that the morphology of the flaky C-S-H crystals exists in all RHA blended cement paste. The morphology of CSH crystals in blended cement paste can be explained by the combined effects of chloride and sulfate ions in seawater environment. The presence of all the formations was confirmed by TGA/DTA and XRD analysis.

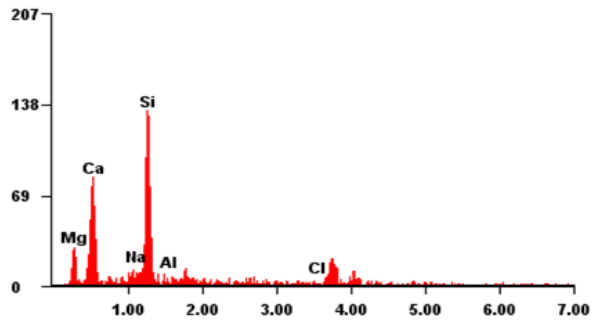


Fig. 6 EDX analysis of RHA cement paste under seawater

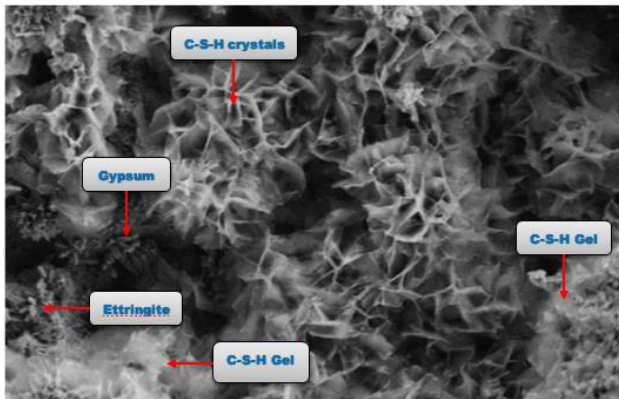


Fig. 7 Morphology of RHA cement paste under seawater

## 5. Summary

From the experiment, it was found that RHA can be satisfactorily used as a cement replacement material in order to increase the durability of concrete under seawater attack. The results also indicate that the amount of  $\text{Ca}(\text{OH})_2$  in the RHA blended cement was lower than that of Portland cement due to the pozzolanic reaction of RHA. Finally, the combination of DTA/TGA, XRD and SEM analysis leads to the positive identification of Friedels Salt ( $\text{Ca}_2\text{Al}(\text{OH})_6(\text{Cl}, \text{OH}) \cdot 2\text{H}_2\text{O}$ ), Ettringite ( $\text{Ca}_6\text{Al}_2(\text{SO}_4)_3(\text{OH})_{12} \cdot 26\text{H}_2\text{O}$ ), Gypsum ( $\text{CaSO}_4 \cdot 2\text{H}_2\text{O}$ ), Calcium Hydroxide ( $\text{Ca}(\text{OH})_2$ ), Brucite ( $\text{Mg}(\text{OH})_2$ ), and other chemical substance formations in specimen.

## Acknowledgements

The support provided by Malaysian Ministry of Higher Education and Universiti Teknologi Malaysia in the form of a research grant vote number Q.J130000.2522.18H05 and Q.J130000.2522.17H69 for this study is highly appreciated.

## References

[1] Memon, A. H., Radin, S. S., Zain, M. F. M. & Trottier, J-F. Effects of mineral and chemical admixtures on high-strength concrete in seawater. *Cement and Concrete Research*. Volume 32, (2002), pp. 373–377.

[2] Abdelkader, S. M., Pozo, E. R. & Terrades, A. M. Evolution of microstructure and mechanical behavior of concretes utilized in marine environments.

*Materials and Design*, Volume 31, (2010), pp. 3412–3418.

[3] Abdulrahman, A., Latiff, A.A.A., Daud, Z., Ridzuan, M.B. & Jagaba, A.H., Preparation and Characterization of Activated Cow Bone Powder for the Adsorption of Cadmium from Palm Oil Mill Effluent. *IOP Conference Series: Materials Science and Engineering*. Volume 136(1), (2016), 012045.

[4] Daud, Z., Awang, H., Kassim, A.S.M., Hatta, M.Z.M. & Aripin, A.M., Comparison of pineapple leaf and cassava peel by chemical properties and morphology characterization. *Advanced Materials Research*. Volume 974, (2014), pp. 384-388.

[5] Islam, M. M., Islam, M. S., Mondal, B. C. & Islam, M. R. Strength behavior of concrete using slag with cement in sea water environment. *Journal of Civil Engineering*, Volume 38, (2010), pp. 129-140.

[6] Marchand, J., Samson, E., Maltais, Y. & Beaudoin, J. J. Theoretical analysis of the effect of weak sodium sulfate solutions on the durability of concrete. *Cement and Concrete Composites*, Volume 24, (2002), pp. 317–329.

[7] Tareq, U. M. & Hidenori, H. Durability of concrete made with different water reducing chemical admixture in tidal environment. *ACI Materials Journal*, Volume 100, (2003), pp. 194-201.

[8] Wu, Z. & Naik, T. R. Chemically activated blended cements. *ACI Materials Journal*, Volume 100, (2003), pp. 434-439.

[9] Hussin, M. W., Nor Hasanah, A. S. L., Abdul Rahman, M. S., Mostafa, S., Mohamed, A. I., Nur Farhayu, A., Nur Hafizah, A. K., Muhd Zaimi, A. M., Jahangir, M. & Habeeb, L. Long term studies on compressive strength of high volume nano palm oil fuel ash mortar mixes. *Jurnal Teknologi (Sciences & Engineering)*, Volume 77, (2015), pp. 15–20.

[10] Ganjian, E. & Pouya, H. S. Effect of magnesium and sulfate ions on durability of silica fume blended mixes exposed to the seawater tidal zone. *Cement and Concrete Research*, Volume 35, (2005), pp. 1332–1343.

[11] BS EN 197-1:2011. Cement. Composition, specifications and conformity criteria for common cements. British European Standard. London, United Kingdom.

[12] ASTM C618-15. Standard Specification for Coal Fly Ash and Raw or Calcined Natural Pozzolan for Use in Concrete. American Society for Testing and Materials, West Conshohocken, PA 19428-2959, United States.

[13] ASTM C311 / C311M-17. Standard Test Methods for Sampling and Testing Fly Ash or Natural Pozzolans for Use in Portland-Cement Concrete. American Society for Testing and Materials, West Conshohocken, PA 19428-2959, United States.

[14] BS EN 13925-1:2003. Non-destructive testing. X-ray diffraction from polycrystalline and amorphous materials. General principles. British European Standard. London, United Kingdom.



- [15] Santhanam, M., Cohen, M. D. & Olek, J. Mechanism of sulfate attack: a fresh look Part 1. Summary of experimental results, *Cement and Concrete Research*, Volume 32, (2002), pp. 915–921.
- [16] Li, D., Chen, Y., Shen, J., Su, J. & Wu, X. The influence of alkalinity on activation and microstructure of fly ash. *Cement and Concrete Research*, Volume 30, (2000), pp. 881-886.
- [17] Vedalakshmi, R., Sundara Raj, A. & Palaniswamy, N. (2008) Identification of various chemical phenomena in concrete using thermal analysis. *Indian Journal of Chemical Technology*, Volume 15, (2008), pp.388-396.